05,13

Formation of exchange bias and shape anisotropy in microobjects based on spin valves

© A.A. Germizina[1], L.I. Naumova[1,2], M.A. Milyaev[1,2], R.S. Zavornitsyn[1,2], A.Yu. Pavlova[1], I.K. Maksimova[1], V.V. Proglyado[1], I.Yu. Kamensky[1], V.V. Ustinov[1,2]

[1] M.N. Mikheev Institute of Metal Physics, Ural Branch, Russian Academy of Sciences, Yekaterinburg, Russia
[2] Institute of Natural Sciences and Mathematics, Ural Federal University, Yekaterinburg, Russia
E-mail: germizina@imp.uran.ru

Received May 3, 2023
Revised May 3, 2023
Accepted May 4, 2023

Rhombus-shaped microobjects formed by strips of two micrometers wide were fabricated from the spin valve film. The influence of the shape anisotropy on the layers magnetic moment rotation during the spin valve magnetic reversal is studied. A method for two-stage thermomagnetic treatment in a direction-fixed magnetic field has been found. The method allows to obtain the opposite sign values of the exchange bias fields in the non-parallel rhombus sides. The direction of the formed exchange bias is determined by the deviation of the strip from the uniaxial anisotropy axis and from the magnetic field applied during thermomagnetic treatment. Based on a rhombus-shaped microobject made from a single spin valve film, the device is a Full Wheatstone bridge. Each side of the rhombus is an active magnetically sensitive element.

Keywords: spin valve, exchange bias, shape anisotropy, Wheatstone bridge, microobject.

DOI: 10.61011/PSS.2023.08.56574.76

1. Introduction

Spin valve type nanostructures have a giant magnetoresistance effect, well reproducible by consistently high magnetoresistance and high magnetoresistive sensitivity in weak fields. These characteristics allow the use of spin valves in magnetic field sensors [1,2].

The spin valve is a multilayer structure that includes two ferromagnetic (FM) layers separated by a non-magnetic copper layer, an antiferromagnetic (AFM) layer, buffer and protective layers. One of the FM-layers, called fixed, is located next to the antiferromagnetic and is connected to it by an exchange interaction. As a result, unidirectional magnetic anisotropy occurs with the axis of unidirectional anisotropy (PD). The loop of the magnetization reversal hysteresis of the fixed layer is shifted to the region of large fields. The magnitude of the shift field (H_{ex}) characterizes the exchange interaction at the FM/AFM boundary. The second FM-layer is called free and is magnetized in small fields. The shift of the low-field hysteresis loop (H_{j}) is determined by the characteristic interaction field of FM-layers separated by a layer of copper [3]. Upon sputtering in a magnetic field, a uniaxial anisotropy is formed in the spin valve with an easy magnetic axis (EA) parallel to the magnetic field applied during sputtering. The shape anisotropy [4] is of great importance in microobjects.

Often, in a spin valve to expand the operating temperature range, the fixed layer is replaced with a synthetic antiferromagnet — SAF [5,6]. The SAF consists of two FM-layers separated by a ruthenium layer and bound by an antiferromagnetic RKKY interaction. In this case, the ferromagnetic layer adjacent to the antiferromagnet is called fixed, the other FM-layer is a reference layer. SAF at a certain value of the applied field (H_{sf}) goes into a spin-flop state. At $H = H_{\mathrm{sf}}$, the magnetic moments of the fixed ($\mathbf{M}_{\mathrm{p}}$) and the reference ($\mathbf{M}_{\mathrm{r}}$) layers are antiparallel and perpendicular to the applied field. When the applied field decreases ($H < H_{\mathrm{sf}}$) $\mathbf{M}_{\mathrm{p}}$ and $\mathbf{M}_{\mathrm{r}}$ are oriented parallel to $\mathbf{H}$ and antiparallel to each other, and when the field increases ($H > H_{\mathrm{sf}}$) $\mathbf{M}_{\mathrm{p}}$ and $\mathbf{M}_{\mathrm{r}}$ rotate, setting in the direction of $\mathbf{H}$.

The PD direction in the spin valve can be changed by thermomagnetic treatment (TMT). TMT consists of heating the spin valve to a temperature exceeding than the blocking temperature (T_{b}), at which the field H_{ex} tends to zero, and subsequent cooling. Upon cooling, PD is formed again and coincides with the direction of the magnetic moment $\mathbf{M}_{\mathrm{p}}$ of the fixed FM-layer.

When designing various electronic devices, the work of which is associated with fixing changes in the magnetic field and measuring its magnitude, magnetically sensitive elements are often connected in accordance with the electrical circuit of the Wheatstone bridge [7–11]. This allows avoiding a temperature drift, reducing noise and obtaining an output signal which is symmetrical with respect to $H = 0$ [10]. The principle of operation of the Wheatstone bridge is based on measuring the potential difference (U_{out}) between the average terminals of two parallel branches. In each branch, two magnetically sensitive elements (arms) are connected in series. The maximum ratio between the applied to the bridge branches (U_{in}) and U_{out} is obtained if the electrical resistance increases in the two arms of the bridge, and decreases in the other two ones in case of any change of the magnetic field. Such a scheme with four active elements is called a full Wheatstone bridge.

If the active elements of the Wheatstone bridge are spin valves, then their PD should be mutually pairwise opposite. The following techniques are used to obtain the required PD orientation: two-stage sequential sputtering of spin valves with different directions PD [12] and EA [13] or with a different composition [14] on the corresponding parts of the substrate; conducting TMT in the field corresponding to the spin-flop the state in the SAF [6,13]; the use of a permanent magnet to create additional oppositely directed components of the field in the active elements of the bridge [11].

Earlier, we proposed in the work [13] a method for the formation of a pairwise opposite exchange shift and perpendicular mutual arrangement of PD and EA in the spin-valve elements of the Wheatstone bridge. The technique consisted in two-stage sputtering of the spin valve film on the corresponding parts of the substrate to obtain mutually perpendicular directions EA and subsequent three-stage TMT using the spin-flop transition field H_{sf}.

In this paper, the features of the magnetization reversal of spin valves due to a combination of shape anisotropy, unidirectional and uniaxial anisotropy and the effect of shape anisotropy on changes in exchange displacement during thermomagnetic processing of micro-objects based on spin valves are investigated. Taking into account the data obtained, a technique for the formation of a pairwise opposite exchange bias with a small angle of deviation PD from EA in the spin-valve elements of the Wheatstone bridge is found.

2. Experiment

Spin valves compositions
$Ta(5\,nm)/[Ni_{80}Fe_{20}]_{60}Cr_{40}(5\,nm)/Co_{70}Fe_{20}Ni_{10}(t_{FMF})/Cu(t_{Cu})/Co_{70}Fe_{20}Ni_{10}(t_{FMR})/Ru(0.8\,nm)/Co_{70}Fe_{20}Ni_{10}(t_{FMP})/Fe_{50}Mn_{50}(t_{AFM})/Ta(6\,nm)$ are made by magnetron sputtering at room temperature on glass substrates 25×25 mm. During sputtering, a magnetic field with a strength of $H = 80$ Oe was applied in the plane of the substrate. The three-layer structure of $Co_{70}Fe_{20}Ni_{10}/Ru/Co_{70}Fe_{20}Ni_{10}$ is a synthetic antiferromagnet.

The thicknesses of the layers are indicated in nanometers. The thickness of the copper layer $t_{\mathrm{Cu}} = 2$, 2.1 and 2.4 nm, at the thicknesses of the free FM-layer $t_{\mathrm{FMF}} = 3.5$ and 4 nm, reference FM-layer $t_{\mathrm{FMR}} = 3.1$, 3.5, 4 and 4.3 nm, fixed FM-layer $t_{\mathrm{FMP}} = 3$ and 3.3 nm and AFM-layer $t_{\mathrm{AFM}} = 10$ and 11 nm.

The method of mask-free laser lithography using the DWL 66+ unit manufactured by Heidelberg Instruments Mikrotechnik GmbH was used for the manufacture of micro-objects. The following three types of micro-objects were manufactured. (1) Microstrips of width $w = 1$, 4 and 6 μm whose long side is parallel to EA. (2) V-shaped objects representing two angle-forming microstrips with copper contact pads at the top of the corner and at the ends of the microstrips. The magnitude of the angle is 20, 40 and 60°, and its bisector coincides with EA (Fig. 1, *a*). (3) Rhombus-shaped micro-objects (Fig. 1, *b*) with copper contact tracks at the corners. The sides of the rhombus are microstrips 315 μm long and 2 μm wide. The angle at the top of the rhombus is 40°. EA is directed along the long diagonal of the rhombus. This micro-object is designed to implement the electrical circuit of the Wheatstone Bridge. Contact pads and tracks were made using a lift-off procedure.

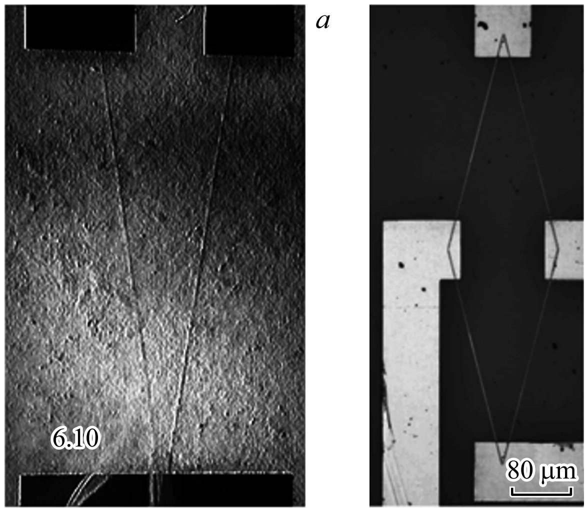

Figure 1. Photos of micro-objects: *a* — sample V-shape. The width of the microstrips $w = 6\,\mu$m, the angle between the microstrips and EA 10°; *b* — a rhombus-shaped microobject.

Magnetoresistance measurements and TMT were carried out in an unit assembled on the basis of a Bruker electromagnet and a LakeShore 336 temperature controller. The resistance was measured by a four-point probe method with a constant current flowing in the plane of the film. Magnetoresistance was determined as

$$\Delta R/R_s = \big(R(H) - R_s\big)/R_s,$$

where $R(H)$ is the resistance of the sample in the magnetic field and R_s is the resistance in the saturation field (H_{sat}). In the TMT process, annealing was conducted in a helium atmosphere at a temperature $T_{\mathrm{TMT}} = 448$ K, exceeding the blocking temperature T_{b}, which for spin valves with SAF based on antiferromagnetic alloy FeMn is $T_b = 423-433$ K [5].

An automated vibration magnetometer was used for magnetic measurements.

When measuring the dependence of the output voltage on the applied field of the Wheatstone bridge, a constant voltage $U_{\mathrm{in}} = 5$ V was applied to the contact pads at the sharp corners of the rhombus. The measured signal $U_{\mathrm{out}}(H)$ was removed from the contact pads in the obtuse corners of the rhombus.

3. Results and discussion

3.1. Effect of shape anisotropy on remagnetization of spin valves

To identify the effect of the sample size and shape on the magnetization reversal of spin valves, the field dependences of magnetoresistance for microstrips of different widths were measured. Figure 2, *a* shows magnetoresistive curves for microstrips $w = 6$ and $1\,\mu$m, measured in a field applied parallel to PD $\|$ EA and the long side microstrips. At $w = 1\,\mu$m, the width of the low-field loop characterizing the magnetization reversal hysteresis of the free layer is greater than at $w = 6\,\mu$m. The obtained magnetoresistive curves are very close for the rest of the parameters.

When discussing the measurement results, we will use the interaction between the layers in the spin valve and changes in its magnetoresistance to understand the orientation of the magnetic moments of the free, reference and fixed layers.

It is known that the dependence of the spin valve resistance on the angle (φ) between the magnetic moments of the free layer $\mathbf{M}_\mathrm{f}$ and the reference layer $\mathbf{M}_\mathrm{r}$ is described by the expression

$$R(\phi) = R_\mathrm{P} + (R_\mathrm{AP} - R_\mathrm{P})(1 - \cos\phi)/2, \tag{1}$$

where R_P and R_AP is the spin valve resistances in the co-directional and counter-directional state $\mathbf{M}_\mathrm{f}$ and $\mathbf{M}_\mathrm{r}$.

The maximum magnetoresistance $(\Delta R/R_\mathrm{s})_\mathrm{max}(\|)$ (Fig. 2, *a*) corresponds to $\varphi = 180^\circ$ and is 10.8 and 11.3% at $w = 1$ and $6\,\mu$m.

Fig. 2, *b* shows the field dependence of the magnetoresistance obtained in a field applied perpendicular to PD for a microstrip $w = 6\,\mu$m. The dependences obtained for $w = 4$ and $6\,\mu$m $(\Delta R/R_\mathrm{s})(H)$ are typical for spin valves when measured in the field $\mathbf{H} \perp$ PD. Namely, the maximum magnetoresistance is $(\Delta R/R_\mathrm{s})_\mathrm{max}(\perp) \approx 0.5(\Delta R/R_\mathrm{s})_\mathrm{max}(\|)$, which corresponds to $\varphi \approx 90^\circ$ [15].

For a microstrip with a width of $w = 1\,\mu$m, the magnetoresistive curve looks completely different (Fig. 2, *c*). In particular, on the descending branch of the hysteresis loop, the magnetoresistance reaches a value

$$(\Delta R/R_\mathrm{s})_\mathrm{max}(\perp) \approx (\Delta R/R_\mathrm{s})_\mathrm{max}(\|),$$

of $\varphi \approx 180^\circ$, respectively.

During remagnetization, the following changes occur in the direction of the magnetic moments of the free, reference and fixed layers of the spin valve. When the applied field is $H \geq H_\mathrm{sat}$, the magnetic moments $\mathbf{M}_\mathrm{f}$, $\mathbf{M}_\mathrm{r}$ and the magnetic moment of the fixed layer $\mathbf{M}_\mathrm{p}$ are co-directional and parallel the field, and the magnetoresistance is minimal. When the applied field decreases, $\mathbf{M}_\mathrm{r}$ and $\mathbf{M}_\mathrm{p}$, turn antiparallel to each other due to the exchange interaction through the ruthenium layer, and then orient along PD due to the interaction at the FM/AFM boundary. This results in an increase of the angle φ and magnetoresistance.

Fig. 3 shows the region of small fields for magnetoresistive curves (Fig. 2, *b, c*) obtained for microstrips of width $w = 1$ and $6\,\mu$m, as well as orientation $\mathbf{M}_\mathrm{f}$ and $\mathbf{M}_\mathrm{r}$.

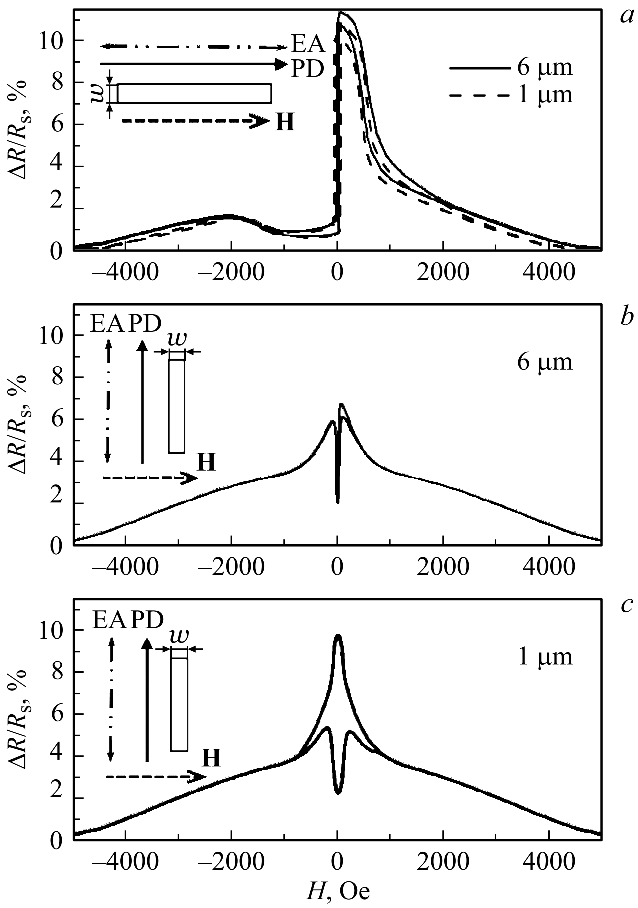

Figure 2. Field dependences of magnetoresistance for spin valve microstrips Ta(5)/NiFeCr(5)/CoFeNi(4)/Cu(2.1)/CoFeNi(4)/Ru(0.8)/CoFeNi(3)/FeMn(10)/Ta(5) ($w = 6$ and $1\,\mu$m). Inserts: the direction of EA and PD with respect to the microstrip and the applied field.

A change in the field corresponding to an ascending or descending branch of the hysteresis loop causes a clockwise or counterclockwise half-turn of the moment $\mathbf{M}_\mathrm{f}$ at $w = 6\,\mu$m. For samples with $w = 1\,\mu$m, similar changes in the magnetic field lead to fundamentally different changes, namely, $\mathbf{M}_\mathrm{f}$ makes a complete revolution in the plane of the film around the normal to it. To implement such a remagnetization mechanism, it is necessary that the rotation of the magnetic moment in one direction, for example, counterclockwise, is energetically more advantageous. Apparently, such conditions are realized in the presence of a small angle (β) deviation from the parallel mutual orientation of PD $\|$ EA and the long side of the microstrip, as shown in Fig. 3 for the case of $w = 1\,\mu$m. The occurrence of this deviation is very likely during the lithographic manufacture of micro-objects.

In small fields, the shape anisotropy affects the orientation of the magnetic moments of the layers, so $\mathbf{M}_\mathrm{f}$, $\mathbf{M}_\mathrm{r}$ and $\mathbf{M}_\mathrm{p}$ tend to line up along the microstrip at its small width.

Figure 4 shows the low-field parts of the magnetic hysteresis loops measured in a field applied parallel and

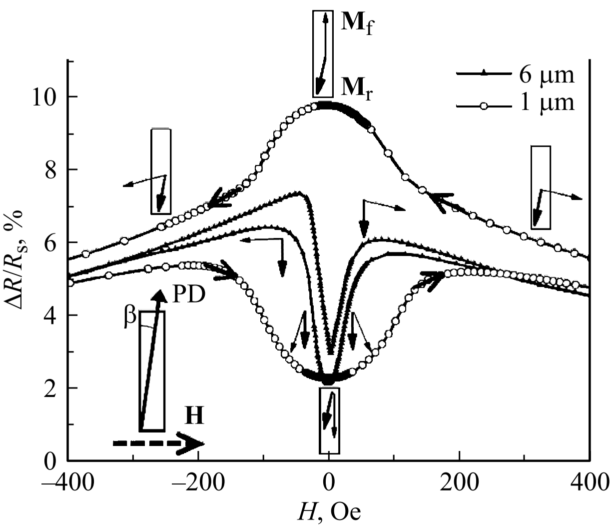

Figure 3. The region of small fields for magnetoresistive curves (Fig. 2, *b, c*). The arrows on the magnetoresistive curve indicate the direction of change in the magnetic field during measurement. Inserts: the direction of PD and fields relative to the microstrip, the direction of magnetic moments $\mathbf{M}_f$ and $\mathbf{M}_r$.

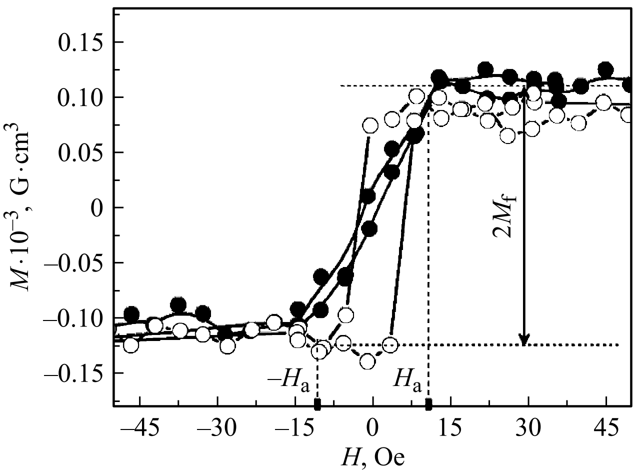

Figure 4. Magnetic hysteresis loops of the spin valve Ta(5)/NiFeCr(5)/CoFeNi(4)/Cu(2.1)/CoFeNi(4)/Ru(0.8)/CoFeNi(3)/FeMn(10)/Ta(6) obtained in small fields when applied fields along (line with empty characters) and perpendicular (line with filled characters) EA.

perpendicular to the EA spin valve. The values of the effective uniaxial anisotropy field (H_a) and the magnetic moment of the free layer were estimated as shown in the figure.

The effective anisotropy field of the shape can be estimated using the expression [16]:

$$H_{sh} = 4\pi M_s t_{FM}/w, \quad (2)$$

where M_s — spontaneous magnetization, t_{FM} — ferromagnetic layer thickness, w — width microstrips.

We estimate the value of spontaneous magnetization as $M_s \approx M_f/V_{FMF} \approx 480$ G, where V_{FMF} — the volume of the free layer. Then, with the thickness of the free ferromagnetic layer $t_{FMF} = 4$ nm and the width of the strip $w = 1\,\mu$m, it is possible to estimate the value of $H_{sh} = 24.1$ Oe, respectively, at $w = 6\,\mu$m $H_{sh} = 4$ Oe. The effective uniaxial anisotropy field for a spin valve of such a composition is $H_a \approx 10$ Oe (Fig. 4).

For microstrips with a width of $w = 1\,\mu$m $H_{sh} > H_a$. Then, at $H \approx 0$, for the magnetic moments of the fixed, reference and free layers, the orientation along the microstrip, and not along EA, will be energetically advantageous.

Thus, with a small width of the microstrip, it becomes possible to control the remagnetization of $\mathbf{M}_f$ and the associated exchange interactions $\mathbf{M}_r$ and $\mathbf{M}_p$ by changing the magnitude of the magnetic field and the angle of its deviation from the long side of the micro-object.

3.2. Formation of non-collinear axes of unidirectional anisotropy in microstrips deviated from each other during thermomagnetic processing

The following series of experiments were carried out on V-shaped micro-objects with the width of microstrips $w = 1$, 6 and $8\,\mu$m, deflected in different directions from EA at angles 10, 20 and 30°. It was shown above that at $H \approx 0$ the anisotropy of the shape and the deviation of the microstrips from the applied magnetic field affect the rotation of the magnetic moments of the spin valve layers during magnetization reversal. It can be assumed that for a certain small value of the applied field, the directions of the magnetic moments $\mathbf{M}_p$ in the microstrips will be significantly different, despite the fact that the V-shaped microobject is made of a single film and, accordingly, the composition of the spin valve in the two microstrips is the same. If TMT is produced in this field, then at $T > T_b$, the exchange interaction between the fixed FM and AFM layer will collapse, and then, when cooled in a magnetic field, it will form again, setting new directions PD1 and PD2 in microstrips. It is important that PD1 and PD2 will be co-directed with $\mathbf{M}_p$ at the time of TMT, i.e. not co-directed with each other.

The objective of this stage of research was to form the axes of unidirectional anisotropy PD1 and PD2 in two microstrips of the V-shaped sample so that the angle between PD1 and PD2 was close to 180°.

TMT was performed in a magnetic field H_{TMT} applied perpendicular to the bisector of the angle between the microstrips and, consequently, $\mathbf{H}_{TMT} \perp$ EA. TMT consisted of the following two stages. (I) Heating to the temperature $T_{TMT} = 445$ K, annealing for 10 minutes and cooling to room temperature in a magnetic field $H_{TMT} \approx 9$ kOe, ($H_{TMT} > H_{sat}$). At the same time, new PD co-directed with $\mathbf{H}_{TMT}$ are formed in the microstrips (Fig. 5, *a*, fragment 2). (II) Heating and cooling in a magnetic field as close as possible to $H = 0$. In such a field at $T > T_b$, the magnetic moments $\mathbf{M}_f$, $\mathbf{M}_r$ and $\mathbf{M}_p$ are oriented parallel to EA or along the microstrip, depending on the ratio

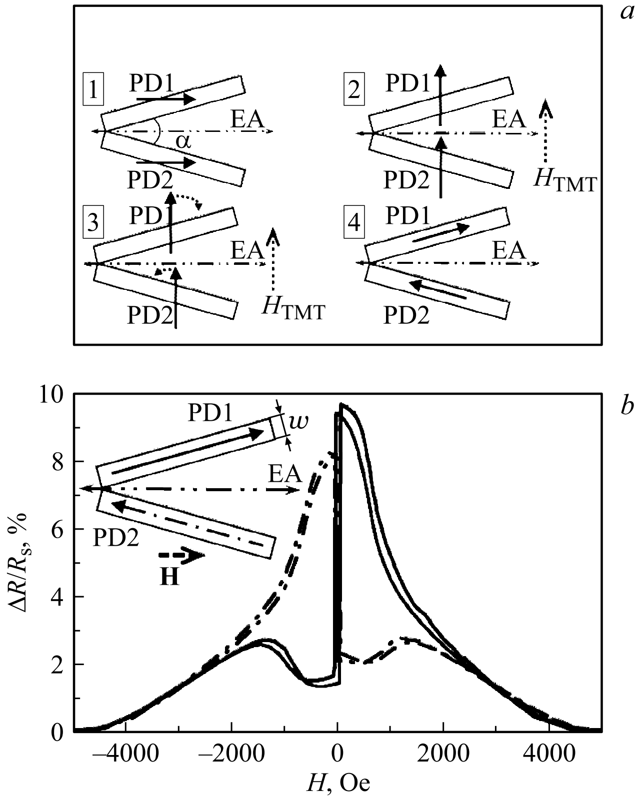

Figure 5. *a* — TMT stages with designated directions EA, TMT fields, PD1 and PD2, *b* — field dependences of magnetoresistance for microstrips ($w = 1\,\mu$m) of spin valve Ta(5)/NiFeCr(5)/CoFeNi(3.5)/Cu(2)/CoFeNi(3.1)/Ru(0.8)/CoFeNi(3.3)/FeMn(11)/Ta(6) deviated from EA by 10°, removed after TMT. Insert: directions EA, PD1 and PD2 and the field applied when measuring magnetoresistive curves.

between the values of the fields H_a and H_{sh}. If $H_{sh} > H_a$, then the associated RKKY interaction $\mathbf{M}_r$ and $\mathbf{M}_p$ in both microstrips line up along them. Making an energetically more advantageous turn at a smaller angle, the magnetic moments in one microstrip of the V-shape sample turn clockwise, and in the other — counterclockwise. For example, if the microstrips are deviated from each other by 20°, then the angle between $\mathbf{M}_p$ in different microstrips will be close to 160°. Further cooling to room temperature leads to the formation of PD1 and PD2 axes in microstrips, co-directed with $\mathbf{M}_p$ (Fig. 5, *a*, fragments 3 and 4).

Fig. 5, *b* shows the field dependences of the magnetoresistance for two microstrips of a V-shape sample, measured in a field applied in parallel to EA after TMT. The nature of the obtained magnetoresistive curves indicates that the projection of PD1 on the applied magnetic field is positive, and in the projection of PD2 is negative. The effect is observed for microstrips of width $w = 1$, 6 and $8\,\mu$m. The angle of deviation of the formed PD1 and PD2 from EA spin valve is equal to the angle of deviation of the microstrip from EA and for different samples is 10, 20 or 30°. Accordingly, the magnetoresistive curves obtained after TMT are characterized by a sharp change in magnetoresistance in small fields and a large width of the low-field hysteresis loop.

The two-stage TMT procedure described above was applied to V-shaped samples with different thicknesses of the copper layer in the spin valve $t_{Cu} = 2$ and 2.4 nm. When changing t_{Cu}, the slope, width and shift of the low-field hysteresis loop of the magnetoresistance of the spin valve [3] change. The low-field parts of magnetoresistive curves obtained after TMT for different microstrips of V-shaped samples are shown in Fig. 6.

For a sample with a copper layer thickness of 2 nm, the low-field hysteresis loops have a smaller displacement from $H = 0$, a smaller slope and a smaller width. In this case, it is important that the hysteresis loops obtained from different microstrips of the V-shape sample are closer to each other. Accordingly, at $t_{Cu} = 2$ nm, the magnetic moments $\mathbf{M}_f$ in one and the other microstrip, when the spin valve is magnetized, turn in opposite directions in very close fields. It is precisely this coordinated rotation $\mathbf{M}_f$ that is preferable when combining spin valve microstrips in accordance with the Wheatstone full bridge scheme.

Thus, both microstrips of the V-shape sample were subjected to a single two-stage TMT in a direction-fixed magnetic field and, nevertheless, new directions PD1 and PD2 were formed in the microstrips, deployed from each

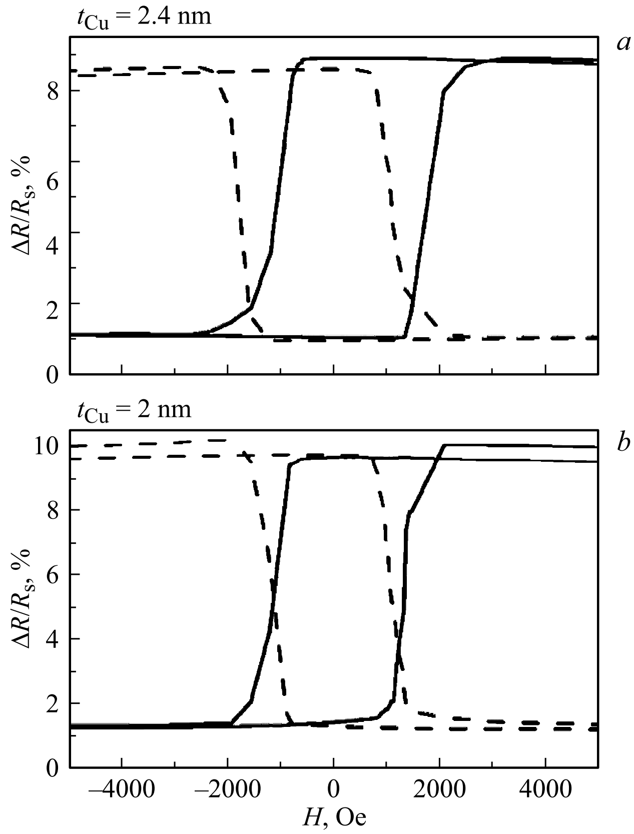

Figure 6. Low-field parts of magnetoresistive curves microstrip of V-shaped samples formed from spin valves with different copper layer thickness 2.4 and 2 nm obtained after TMT.

other at an angle close to 180°. The factors determining the directions of the new PD1 and PD2 are the anisotropy of the shape and the angles of deviation of the microstrip from EA and from the magnetic field applied at TMT.

3.3. Implementation of a Full Wheatstone bridge scheme by a single thermomagnetic treatment

The TMT mode described above was used to form pairwise opposite PD directions in the elements of the Wheatstone Bridge. A rhombus-shaped micro-object is similar to two combined V-shape samples. At the same time, two microstrips are deflected from EA in one direction, and two are deflected in the other direction. After carrying out the TMT procedure described above, new pairwise opposite PD were formed in the magnetic field $\mathbf{H}_{\mathrm{TMT}} \perp \mathrm{EA}$ applied along the short diagonal of the rhombus in the microstrips of the spin valves forming the sides of the rhombus.

Figure 7, *a* shows the dependence of the output voltage of the Wheatstone bridge with a microstrip width of $2\,\mu$m and the angle at the top of the rhombus 40° on the applied magnetic field. The field during the measurement was applied along the long diagonal of the rhombus. Supply voltage $U_{\mathrm{in}} = 5$ V. The width of the hysteresis loop is 43 Oe, sensitivity to magnetic field changes — 3 mV/V/Oe. The sharp dependence of the magnetoresistance on the field and the presence of hysteresis are characteristic of spin valves with a small deviation of PD from EA.

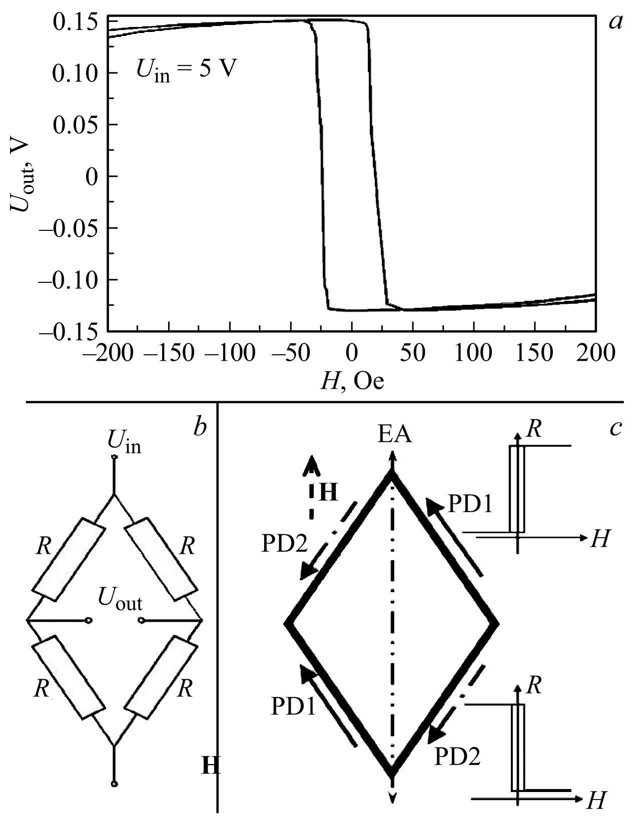

Figure 7. *a* — dependence of the voltage U_{out} on the magnetic field, *b* — electrical diagram of the Wheatstone bridge, *c* — diagram of the Wheatstone bridge with the preferred direction PD of the spin valve in each arm and the corresponding field dependences of magnetoresistance.

In the full Wheatstone bridge, the scheme of which is shown in Fig. 7, *b*, each of the four elements has a resistance R, which in the magnetic field changes by the value ΔR. The ratio between U_{in} and the value of the output signal U_{out} can be estimated as [13]:

$$U_{\mathrm{out}} = U_{\mathrm{in}} \Delta R / R. \tag{3}$$

In the Wheatstone bridge obtained, the ratio $U_{\mathrm{out}}/U_{\mathrm{in}} = 0.06$ does not reach the maximum possible for the spin valves used $(\Delta R/R_{\mathrm{s}})_{\max} = 0.08$. The field applied during the measurement is deflected by 20 degrees from the PD direction in all the spin-valve elements of the bridge, respectively, the angle φ between $\mathbf{M}_{\mathrm{f}}$ and $\mathbf{M}_{\mathrm{r}}$ in weak fields are about 160 degrees (Fig. 7, *c*). Using the expression (1), we obtain for the magnetoresistance the value $\Delta R/R_{\mathrm{s}} = 0.07$, which is close to $U_{\mathrm{out}}/U_{\mathrm{in}} = 0.06$. The performed estimates suggest that after the TMT procedure described above, a magnetic phase with an undesirable PD direction is present in a very small amount in spin-valve elements.

4. Conclusion

It is shown that in weak magnetic fields with a small width of the microstrip, the shape anisotropy can control the rotation of the magnetic moments of the layers during the magnetization reversal of the spin valve.

A thermomagnetic treatment mode is found that forms pairwise opposite axes of unidirectional anisotropy in the sides of a rhombus-shaped microobject based on a spin valve. If the easy magnetic axis coincides with the larger diagonal of the rhombus, and the field during thermomagnetic processing is directed along a smaller diagonal, then opposite exchange shift fields are formed in the non-parallel sides of the rhombus.

The sensor, which is a Full Wheatstone bridge, is made of a single spin valve film by forming a rhombus with contact pads by laser lithography and subsequent thermomagnetic processing in a direction-fixed magnetic field.

The field dependence of the sensor output signal has the form of a step, is characterized by high sensitivity to field changes and the presence of hysteresis. Such characteristics are in demand in switching devices.

Funding

The work was carried out within the scope of the state task of the Ministry of Education and Science (topic „Spin“, No. 122021000036-3 and topic „Magnet“, No. 122021000034-9). Magnetic nanostructures and micro-objects were manufactured in the Department of Technologies and Diagnostics of Nanostructures of the CUC of the IMP of the Ural Branch of the RAS.

Conflict of interest

The authors declare that they have no conflict of interest.

References

[1] D. Su, J. Um, J. Moreno, Z. Nemati, K. Srinivasan, J. Chen, M.R.Z. Kouhpanji, D. Shore, K. Wu, J. Kosel, J.F. Modiano, R. Franklin, J.-P. Wang, B. Stadler. Sensors Actuators A **350**, 114115 (2023).
[2] N. Mabarroh, T. Alfansuri, N.A. Wibowo, N.I. Istiqomah, R.M. Tumbelaka, E. Suharyadi. J. Magn. Magn. Mater. *560*, 163645 (2022).
[3] L.I. Naumova, M.A. Milyaev, R.S. Zavornitsyn, A.Yu. Pavlova, I.K. Maksimova, T.P. Krinitsina, T.A. Chernyshova, V.V. Proglyado, V.V. Ustinov. PMM **120**, *7*, 710 (2019). (in Russian).
[4] R.S. Zavornitsyn, L.I. Naumova, M.A. Milyaev, A.Y. Pavlova, I.K. Maksimova, V.V. Proglyado, V.V. Ustinov. J. Phys.: Conf. Ser. **1389**, 012157 (2019).
[5] M.A. Milyaev, L.I. Naumova, V.V. Proglyado, T.A. Chernyshova, D.V. Blagodatkov, I.Yu. Kamensky, V.V. Ustinov. PMM **116**, *11*, 1129 (2015). (in Russian).
[6] Y. Huai, J. Zhang, G.W. Anderson, P. Rana, S. Funada, C.-Y. Hung, M. Zhao, S. Tran. J. Appl. Phys. **85**, *8*, 5528 (1999).
[7] G. Antarnusa, A. Esmawan, P.D. Jayanti, S.R. Fitriani, A. Suherman, E.K. Palupi, R. Umam, Ardimas. J. Magn. Magn. Mater. **563**, 169903 (2022).
[8] E. Suharyadi, T. Alfansuri, L.S. Handriani, N.A. Wibowo1, H. Sabarman. J. Mater. Sci.: Mater. Electron. **32**, 23958 (2021).
[9] S. Yan, Z. Cao, Z. Guo, Z. Zheng, A. Cao, Y. Qi, Q. Leng, W. Zhao. Sensors **18**, *6*, *1832* (2018).
[10] M. Carvalho, P. Ribeiro, V. Romão, S. Cardoso. J. Magn. Magn. Mater. **536**, 168116 (2021).
[11] U.P. Borole, J. Khan, H.C. Barshilia, P. Chowdhury. Sensors Actuators A **332**, 112103 (2021).
[12] P. Freitas, R. Ferreira, S. Cardoso. Proc. IEEE **104**, *10*, 1901 (2016).
[13] M.A. Milyaev, L.I. Naumova, R.S. Zavornitsyn, I.K. Maksimova, A.Yu. Pavlova, V.V. Proglyado, V.V. Ustinov. PMM **121**, *8*, 794 (2020). (in Russian).
[14] R. Ferreira, E. Paz, P. Freitas, J. Ribeiro, J. Germano, L. Sousa. IEEE Trans. Magn. **48**, *11*, 4107 (2012).
[15] M.A. Milyaev, L.I. Naumova, T.A. Chernyshova, V.V. Proglado, N.A. Kulesh, E.I. Patrakov, I.Y. Kamensky, V.V. Ustinov. PMM **117**, *12*, 1227 (2016). (in Russian).
[16] J.A. Osborn. Phys. Rev. **67**, *11–12*, 351 (1945).

Translated by A.Akhtyamov